Physics-informed multiprobe instrument for IFE experiments (PiMIX)

Zhehui (Jeph) Wang (LANL, email: zwang@lanl.gov), Karl Krushelnick (Univ. Michigan), Mark A. Foster (Johns Hopkins Univ.), Jinsong Huang (Univ. North Carolina, Chapel Hill), Renyuan Zhu (Caltech), Eric R. Fossum (Dartmouth), Jifeng Liu (Dartmouth), Frank Alexander (BNL), Abul Azad (LANL), Steve Batha (LANL), Gabriella Carini (BNL), Matthew S. Freeman (LANL), Haixin Huang (BNL), Paul A. Keiter (LANL), John L. Kline (LANL), Wenting Li (LANL), Eric N. Loomis (LANL), David Montgomery (LANL), Nga T. Nguyen-Fotiadis (LANL), Sasikumar Palaniyappan (LANL), Robert E. Reinovsky (LANL), Joshua P. Sauppe (LANL), Jack S. Shlachter (LANL), Sky K. Sjue (LANL), Xin Yue (Dartmouth), Sven C. Vogel (LANL), Bradley T. Wolfe (LANL) and Dmitry A. Yarotski (LANL).

PiMIX aims at generating high-resolution 3D IFE implosion movies, leveraging machine learning, advanced imaging technologies, and heterogeneous data streams.

Topic: **Diagnostics**

For IFE community workshop (virtual), February 22-24, 2022.

Executive Summary The record-setting MJ neutron yield in the recent NIF experiment opened up a new chapter in burning plasma science and technology. Here we discuss new possibilities that leverage this unprecedented regime of high-energy density laboratory plasmas to advance physics-informed multiprobe instrument (PiMIX), data handling and data interpretation capabilities for IFE experiments. In addition to reconstruction of 3D ICF target implosion movies, our goal is to achieve high-resolution density measurement in the range of one to ten microns, ideally with sub-ns temporal resolution to produce the movies of implosion dynamics. PiMIX will combine multiple-energy photon (X-rays and gamma rays, for example) imaging with neutron and proton measurements to achieve higher information yield than individual diagnostics alone. Initial proof-of-principle measurements will leverage existing LANL and collaborating facilities, new detector capabilities through fast scintillators, perovskites, high-speed imaging sensors, and metamaterial structures. Existing and new data will become available for machine-learning algorithm development and validation. Machine learning and especially physics-informed data-driven algorithms will aim at a unified data pipeline for heterogeneous data processing, constrained by physics models, statistics and the compressed sensing framework.

Introduction: High-resolution imaging of the ICF target during implosion is essential to understanding of heating, 3D asymmetries, plasma flows, jets of the ICF implosion and their temporal evolutions, to optimization of the nuclear fusion energy and neutron yield, to validation of hydro codes, and to predictive designs of future IFE experiments that can reliably reproduce the recent record-setting MJ neutron yield NIF experiment. The discrepancies between the models and measurement are well known in NIF and other IFE experiments. One example is included in Fig. 1. Meanwhile, recent advances in high-speed digital imaging sensors, fast scintillators, perovskite materials, in conjunction with the compressed sensing framework, new data-driven algorithms open up new high-resolution imaging possibilities such as physics-informed multiprobe instrument (PiMIX). IFE burning plasmas provide a unique environment for synchronized multiprobe diagnostics, in part due to the coexistence of X-rays, gamma-rays, neutrons and energetic charged particles. Traditionally, different photon and particle signals are measured independently with different instruments.

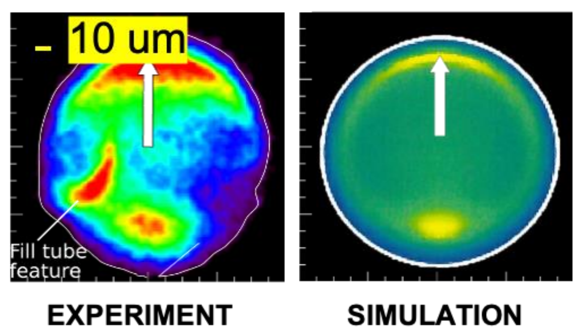

Figure 1. The state-of-the-art imaging techniques in IFE experiments can reveal features and structures around 10 microns. Finer resolutions and 3D information would be very useful to resolve features below these, such as fill tubes. The above image adopted from Ref. [Sch:2021]. The scale bar corresponds to 10 microns.

Metrics: The performance metrics for an IFE instrument may be summarized as the following [Wan:2020]: Spectral response, flux response, detection efficiency, temporal resolution, spatial resolution, data and information content. For a particular detection modality, spectral response is usually described quantitatively by the quantum efficiency as a function of photon or particle energy. Flux response may be described by the dynamic range of the detectors or individual pixels for an array detector. Data and information content include the raw data yield, information yield (mostly achieved in the post-processing pipeline), signal classification and noise rejection. Most

IFE instruments generate 1D or 2D raw data. To characterize 3D asymmetric structures, 3D reconstructions from the 1D and 2D raw data or pre-processed data are necessary. While X-ray instruments have demonstrated nanometer resolution under certain conditions through long signal integration time, repetitive measurements, and the use of monochromatic light, this feat may be hard to reproduce in transient ICF experiments, when the experiments last less than a fraction of one millisecond and are very costly to reproduce. Dynamic imaging in ICF falls to the classification of `flash radiography', one-to-ten-micron spatial resolution in the near future experiments would be superior to the state-of-the-art. The sub-ns resolution is dictated by the need to produce movies of implosion dynamics that can be directly compared with the state-of-the-art hydro codes that run on today's best high-performance computers. Multi-probe capability is a new frontier in IFE instrumentation, enabled by the growing number of instruments and data, and the data-driven algorithms such as deep learning. Physics-informed data science is a new frontier in data science, esp. suited for problems when the amount of data is limited as in most IFE experiments. Compressed sensing framework, which replaces the Nyquist sampling principle, is another approach to achieve high resolution in imaging and 3D reconstruction using sparse data [Can:2006, Don:2006].

Table 1. *A table of metrics for some existing IFE instruments and the new PiMIX concept.*

Metrics	X-ray	Neutron	Gamma-ray	Proton	PiMIX
Physics quantity	Areal density	Ion Temp., Flow, B field	Areal density	Areal density,	Areal density + extra
Detector	Scintillator (indirect)	Scintillator (indirect)	Cherenkov (indirect)	Scintillator (indirect)	Ultrafast silicon, Perovskite (Direct) & scintillator (indirect)
Spatial Resolution	> 10 μm	> 10 μm	> 10 μm	> 100 μm	1-10 μm
Data	homogeneous	homogeneous	homogeneous	homogeneous	heterogeneous
model & interpretation	Physics/ statistics	Physics/ statistics	Physics/ statistics	Physics/ statistics	Physics/statistics + data
3D Reconstruction	Radon	Multi-view		Abel	Sparse algorithms

Technical feasibilities: (Overview) We will build physics-informed multiprobe instrument (PiMIX) based on the emerging framework of data-driven instrumentation, which implements algorithms such as but not limited to a growing number of neural networks using raw data from the sensor arrays. The data-driven framework also allows seamless integration of model-generated data and data from large simulations. The data-driven algorithms will further be constrained by additional physics, the sparse sensing mathematics and statistics. Our interdisciplinary team consists of leading experts from relevant science and technology fields including: sparse and compressed sensing, high-speed sensing materials, imaging sensors, algorithms and data, experiment execution with X-rays, protons, neutrons and other radiographic probes. The three themes of the PiMIX may be summarized as PERFORMANCE, TRANSFORMATION and CONFIRMATION as illustrated in **Figure** 2. Some highlights of the recent progress related to the three themes are given next.

Figure 2. The three themes for a PiMIX instrument development: Performance, Transformation, and Confirmation. Performance goals include 3D reconstruction, high resolution, and ultrafast response time. Based on physics, statistics, and compressed sensing, a number of data transformation techniques will be implemented or developed. Confirmation for multiple radiographic probes in existing LANL and collaborating facilities is also planned.

<u>Novel sensing materials (ultrafast scintillators, Perovskites)</u> Scintillators are widely used in IFE experiments and radiographic imaging. However, most instruments are limited by scintillators that were developed decades ago, which can not meet the increasingly demanding experimental requirements. Two new classes of scintillators are emerging that could significantly outperform the traditional materials. Inorganic scintillators are widely used in HEP experiments to measure photons. Table 2 lists optical and scintillation properties of several inorganic scintillators, characterized at the Caltech HEP Crystal Lab [HEP:2019, Zhu:2021].

Table 2. Optical and scintillation properties of several fast and ultrafast inorganic scintillators [Zhu:2021]. [a] top/bottom row: slow/fast component; [b] at the emission peak; [c] normalized to LYSO:Ce.

	BaF_2	BaF_2:Y	ZnO:Ga	YAP:Yb	YAG:Yb	β-Ga_2O_3	LYSO:Ce	LuAG:Ce	YAP:Ce	GAGG:Ce	LuYAP:Ce	YSO:Ce
Density (g/cm^3)	4.89	4.89	5.67	5.35	4.56	5.94[1]	7.4	6.76	5.35	6.5	7.2[f]	4.44
Melting points (°C)	1280	1280	1975	1870	1940	1725	2050	2060	1870	1850	1930	2070
X_0 (cm)	2.03	2.03	2.51	2.77	3.53	2.51	1.14	1.45	2.77	1.63	1.37	3.10
R_M (cm)	3.1	3.1	2.28	2.4	2.76	2.20	2.07	2.15	2.4	2.20	2.01	2.93
λ_I (cm)	30.7	30.7	22.2	22.4	25.2	20.9	20.9	20.6	22.4	21.5	19.5	27.8
Z_{eff}	51.6	51.6	27.7	31.9	30	28.1	64.8	60.3	31.9	51.8	58.6	33.3
dE/dX (MeV/cm)	6.52	6.52	8.42	8.05	7.01	8.82	9.55	9.22	8.05	8.96	9.82	6.57
λ_{peak}[a] (nm)	300 220	300 220	380	350	350	380	420	520	370	540	385	420
Refractive Index[b]	1.50	1.50	2.1	1.96	1.87	1.97	1.82	1.84	1.96	1.92	1.94	1.78
Normalized Light Yield[a,c]	42 4.8	1.7 4.8	6.6[d]	0.19[d]	0.36[d]	6.5 0.5	100	35[e] 48[e]	9 32	115	16 15	80
Total Light yield (ph/MeV)	13,000	2,000	2,000[d]	57[d]	110[d]	2,100	30,000	25,000[e]	12,000	34,400	10,000	24,000
Decay time[a] (ns)	600 0.5	600 0.5	<1	1.5	4	148 6	40	820 50	191 25	53	1485 36	75
LY in 1[st] ns (photons/MeV)	1200	1200	610[d]	28[d]	24[d]	43	740	240	391	640	125	318
40 keV Att. Leng. (1/e, mm)	0.106	0.106	0.407	0.314	0.439	0.394	0.185	0.251	0.314	0.319	0.214	0.334

Organic-inorganic lead halide perovskites with ABX_3 structure have attracted attention in recent years for ionizing radiation detection due to their short attenuation lengths, high stopping powers, large mobility-lifetime products, tunable bandgaps, simple and low-cost single crystal growth from liquid solution processes. These materials have a large tunability of compositions and thus can meet demanding requirements of multiprobe radiography. The A, B, X sites can be tuned in the bandgap, stopping power, electronic properties, *etc*. to distinguish ionization particles of different energies and species. The very high mobility and especially long carrier recombination lifetime allows long carrier extraction distance, which also enable quick detection. Huang group in UNC pioneered the fabrication of perovskite materials with large mobility-lifetime > 0.01 cm^2/V and carrier diffusion length >1 mm [Don:2015]. Applications of single crystalline halide perovskites for radiation detection [She:2016], growth on silicon and metal surfaces [Wei:2016] have also been demonstrated. The halide perovskites have shown unprecedented defect tolerance important for radiation detection. Radiation-induced point defects do not cause deep trap level in perovskites. The self-recovery of electronic properties after extended storage has also been observed.

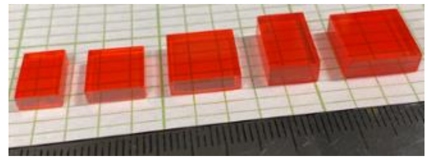

Figure 3. Perovskite single crystals grown (the grids: 1×2 mm) by Huang group at UNC, Chapel Hill.

<u>High-speed imaging sensors</u> The state-of-the-art commercial fast CMOS cameras such as Phantom TMX7510 have a full resolution of 1280 × 800 pixels at 76k frames per second (fps). Fossum's Dartmouth group is currently developing a high-speed continuous-mode image sensor based on a low-cost 180-nm process (TMX 7510 used110-nm process). With a superblocks-wise low-noise readout structure, a novel asynchronous SAR ADC design, and pump-gate global-shuttle pixel. The new Dartmouth sensor can run at 78.1kfps but with much lower total noise than TMX7510. The sensor will have 12 identical superblocks. Each superblock will be self-contained each with its own pixel array, readout circuits, and peripheral supporting circuits. Multiple superblocks can be instantiated on the same chip to configure the sensor resolution easily without sacrificing the frame rate. A 96 ×120 test chip has been designed and taped out, **Figure 4**. Currently, the test sensor frame rate is limited by the slow 180-nm process. With a more advanced process such as 110-nm, the frame rate would increase significantly. In comparison, the highest frame rate burst-mode image sensor, reported by Sugawa/Kuroda's group at Tohoku University, has reached 100 Million fps with 368 frames record length. The key to this burst-mode high-speed performance was the high-density memory process, which formed deep-trench high-density capacitors inside each pixel to store the frames. For scientific instrumentation and niche market, such a unique fabrication process would be either not accessible or too expensive to implement. Dartmouth is therefore pursuing a high-speed burst-mode image sensor fabricated on a regular image sensor process. The target image sensor will run at 10+Mfps with 128+ frames record length. With analog and digital circuit design, pixel charge transfer time, pixel output line RC delay, and control line RC delay can be minimized to achieve 10+Mfps. Currently, there are two candidate methods under verification to store pixel frame information A) in the charge domain, B) the voltage domain. With charge domain methods, multiple storage wells will be formed inside each pixel to temporally save photon-generated electrons and shift them out sequentially during the readout process. With voltage methods, multiple regular MOS caps will be instantiated out of each pixel. RC delay between pixel output line and MOS cap will be carefully calculated and simulated to boost the target sensor frame rate.

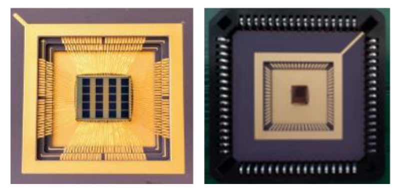

Figure 4. Novel CMOS imaging sensors from the Fossum group at Dartmouth. The one on the left has single-photon sensitivity at room temperature [MaM:2017]. The high-speed sensor prototype on the right has a fraction of the noise of the state-of-the-art commercial sensors.

<u>Machine learning algorithms</u> PiMIX will be enabled by machine learning, mostly through post processing of images, 3D reconstructions and data interpretation. Even though the hardware for

real-time data acquisition and processing will also be available, it will not be necessary since the experimental rep rate is low (< a few times a day for now) and experimental duration will be a faction of 1 ms. Examples of LANL-led work may be found in [Wan:2020a, Wol:2021]. Similar literature is rapid growing from the broad IFE community.

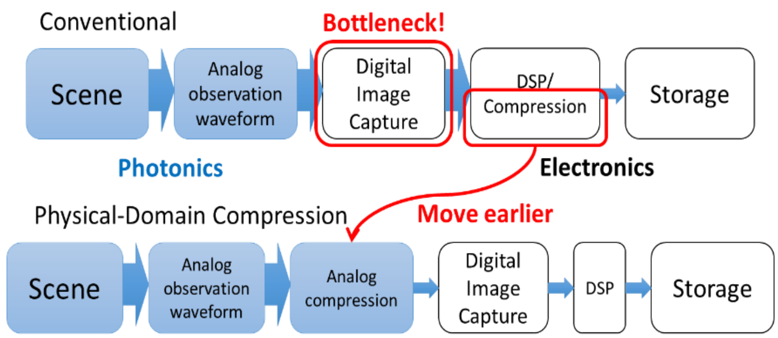

Figure 5. Implementing data compression in the physical (analog) domain alleviates bottlenecks in data capture allowing for the acquisition of a greater amount of quantitative information from ephemeral experiments.

Compressed sensing The Foster group at Johns Hopkins will focus on the development of novel data acquisition schemes that can dramatically increase the amount of information obtained under the extreme conditions encountered in IFE experiments. IFE experiments produce extremely large amounts of transient high-dimensional (space, spectrum, time, etc.) information in the analog domain and conventional diagnostics only capture a fraction of this information due to bottlenecks in data capture and the analog-to-digital conversion process as depicted in **Figure 5**. Several methods will be explored to achieve physical domain or analog data compression [Gao:2014]. Examples of such analog compression include coded apertures, novel optics using metamaterials and phased arrays, and high-speed analog electronics [Bos:2015, Shi:2019, Ale:2020].

Confirmation platforms Even though most of the IFE experiments have a low rep rate (below 1 Hz duty cycle), and correspondingly small data sets that are far from being sufficient for the machine learning algorithms, we will resort to additional laboratory experiments that can generate much larger experimental data sets, and futher augmented by model-driven and simulation-driven data sets for PiMIX. University of Michigan has two high rep rate laser systems: 1) TW scale systems at 500 Hz ; 2) 300 TW system at 5 Hz - both of which can be used for PiMIX development. Other LANL and collaborating facilities include LANSCE, the Advanced Photon Source at Argonne, NSLS-II and AGS GeV protons at Brookhaven. Over a longer term, the PiMIX development through push for more experimental data may also benefit the IFE program towards high-rep-rate operations. Automated system operation and data generation through machine learning techniques will be critical for the experimental tasks and data generation. Bayesian optimization recently allowed the first fully automated control and optimization of a laser-plasma accelerator with up to six independent laser and plasma parameters [Sha:2020]. Future IFE experiments will necessarily have a greater number of laser and experimental parameters that must be optimized. In addition to Bayesian optimization, genetic algorithms and other methods are emerging. Methods will also mature that can account for experimental errors, the uncertainty arising from the sparsity of the data, fluctuations and measurement variances. Through automated optimization, experiments with 10-Hz rep rate at IFE-relevant laser energies may be feasible in the near term.

References:

[Ale:2020] M. Alemohammad, E. R. Wainwright, J. R. Stroud, T. P. Weihs, and M. A. Foster, "Kilohertz frame rate snapshot hyperspectral imaging of metal reactive materials," Appl. Opt. 59, 10406-10415 (2020).

[Bos:2015] B. T. Bosworth, J. R. Stroud, D. N. Tran, T. D. Tran, S. Chin, and M. A. Foster, "High-speed flow microscopy using compressed sensing with ultrafast laser pulses," Opt. Express 23, 10521-10532 (2015).

[Can:2006] E. Candès, J. Romberg, and T. Tao, *IEEE Trans. Inform. Theory* **52**(2) (2006) 489–509; E. Candès and T. Tao, *IEEE Trans. Inform. Theory* 52 (12) (2006) 5406–5425.

[Don:2006] D. L. Donoho, *IEEE Trans. Info. Theory* **52** (2006) 1289-1306.

[Don:2015] Dong, Q.; Fang, Y.; Shao, Y.; Mulligan, P.; Qiu, J.; Cao, L.; Huang, J., Electron-hole diffusion lengths> 175 μm in solution-grown CH3NH3PbI3 single crystals. Science 2015, 347 (6225), 967-970.

[Gao:2014] L. Gao, J. Liang, C. Li, and L. V. Wang, "Single-shot compressed ultrafast photography at one hundred billion frames per second," Nature 516, 74–77 (2014).

[HEP:2019] Report of the DOE Office of Science Workshop on "Basic Research Needs Stydy on HEP Detector Research and Development," Dec 11-14, 2019, https://science.osti.gov/hep/Community-Resources/Reports

[Hoff:2013] N. M. Hoffman et al, *Measurement of areal density in the ablators of inertial-confinement-fusion capsules via detection of ablator (n, n'□) gamma-ray emission, Phys. Plasma.* **20** (2013) 042705.

[MaM:2017] J. Ma, S. Masoodian et al., Optica 4, 1474 (2017).

[Sch:2021] D. J. Schlossberg et al, PRL 127 (2021) 125001.

[Sha:2020] R. J. Shalloo, S. J. D. Dann, J.-N. Gruse, et al, Automation and control of laser wakefield accelerators using Bayesian optimization. Nature Communications 11 (2020) 6355.

[She:2016] Shen, L.; Fang, Y.; Wang, D.; Bai, Y.; Deng, Y.; Wang, M.; Lu, Y.; Huang, J., A Self-Powered, Sub-nanosecond-Response Solution-Processed Hybrid Perovskite Photodetector for Time-Resolved Photoluminescence-Lifetime Detection. Advanced Materials 2016, 28 (48), 10794-10800.

[Shi:2019] J. Shin, D. Tran, S. Chin, T. D. Tran, and M. A. Foster, "A minimally invasive lens-free computational microendoscope," Sci. Adv. 5, eaaw5595 (2019).

[Wan:2020a] Z. Wang, J. Xu, Y. E. Kovach, B.T. Wolfe, E. Thomas Jr, H. Guo, J.E. Foster, Han-Wei Shen, Physics of Plasmas 27 (3) (2020) 033703.

[Wan:2020b] Z. Wang and UDA collaboration, Los Alamos National Laboratory Report LA-UR-20-22210 (2020).

[Wei:2016] Wei, H.; Fang, Y.; Mulligan, P.; Chuirazzi, W.; Fang, H.-H.; Wang, C.; Ecker, B. R.; Gao, Y.; Loi, M. A.; Cao, L.; HUang, J., Sensitive X-ray detectors made of methylammonium lead tribromide perovskite single crystals. Nature Photonics 2016, 10, 333-339.

[Wol:2021] BT Wolfe, Z Han, JS Ben-Benjamin, JL Kline, DS Montgomery, et al, Review of Scientific Instruments 92 (3) (2021) 033547.

[Zhu:2021] R.-Y. Zhu, Invited paper "Progress on Inorganic Scintillators for Future HEP Experiments," doi: 10.1117/12.2596459 (2021).

Summary Slide: (single, later)

[Submission emails: zylstra1@llnl.gov and albrecht5@llnl.gov]